Supporting information

Cooperativity basis for small-molecule stabilization of protein-protein interactions

Pim J. de Vink,[a] Sebastian A. Andrei,[a] Yusuke Higuchi,[b] Christian Ottmann,[a,c] Lech-Gustav Milroy,[a] Luc Brunsveld[a]*

[a.] Laboratory of Chemical Biology, Department of Biomedical Engineering and Institute for Complex Molecular Systems, Eindhoven University of Technology, P.O. Box 513, 5600MB, Eindhoven, The Netherlands.
[b.] The Institute of Scientific and Industrial Research, Osaka University, Ibaraki, Japan.
[c.] Department of Organic Chemistry, University of Duisburg Essen.

Contents

Supporting Figures

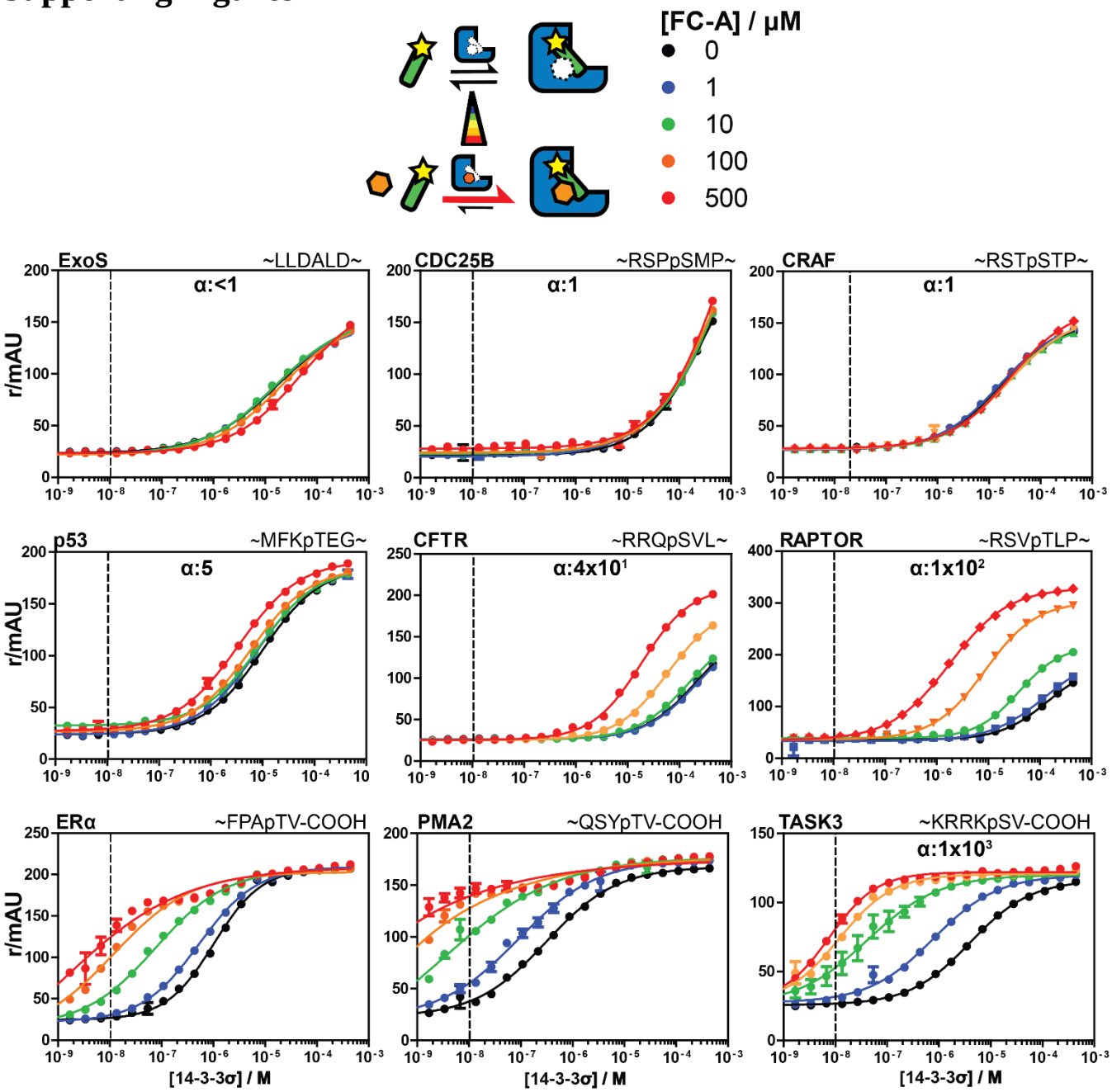

Supporting Figure 1. Fluorescence polarization assays of various 14-3-3 binding-partners. 14-3-3σ is titrated to FITC-labeled 14-3-3 binding peptides (10 nM, indicated by the vertical dashed line) at various concentrations of FC-A between 0 and 500 µM. Experiments are performed as triplicates and errors bars indicate the standard deviations. The cooperativity factor α, defined as the ratio between stabilized affinity and the non-stabilized affinity of the peptide for the receptor, K_D^{I}/ K_D^{III} is obtained though data-fitting according to the model depicted in Supporting Figure 5. The intrinsic affinity of FC-A is determined to be around 300 µM.

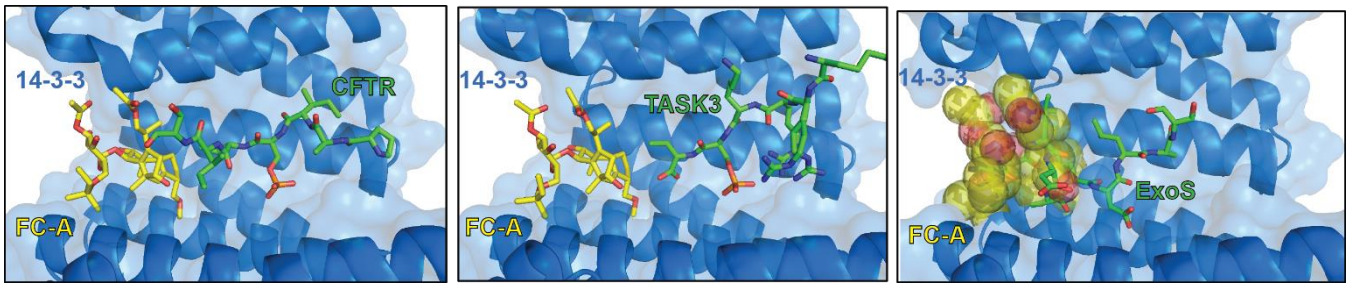

Supporting Figure 2. Structural comparison of CFTR, TASK3 and EXOS-epitopes in complex with 14-3-3 (pdb: 5D3F[1], pdb: 3P1O[2], pdb: 2O02[3])**.**

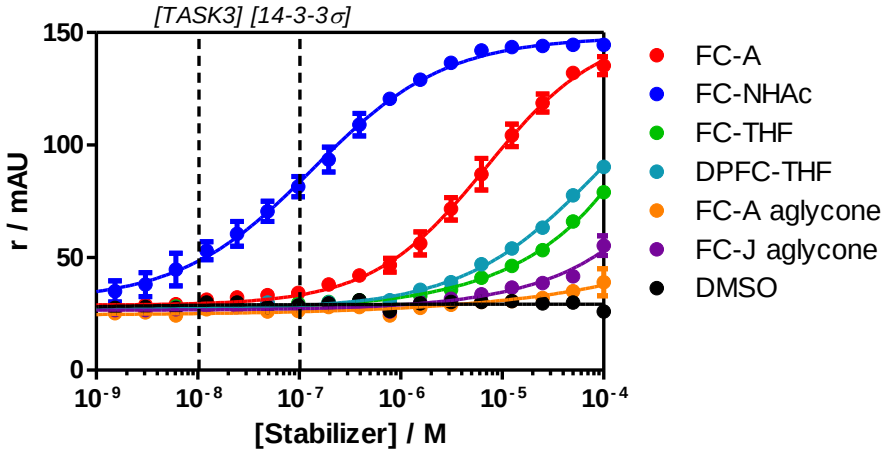

Supporting Figure 3. Direct compound dose-response titrations of different fusicoccin analogs to 10 nM FITC-labelled TASK3 peptide and 100 nM 14-3-3σ, indicated by vertical dashed lines, in FP-Buffer (10 mM HEPES (pH 7.4), 150 mM NaCl with 0.01% (v/v) TWEEN-20, 1% (w/v) BSA and 2% DMSO through-out the assay). Experiments are performed as triplicates and errors bars indicate the standard deviations

Experimental Procedures

General information

Fusicoccin A and J were obtained as a metabolite of *Phomopsis amygdali*. FC-A aglycone and FC-J aglycone[2,4], FC-THF and DP FC-THF[2], and FC-NAc[5] were made according to the corresponding literature procedures. Unless otherwise noted, all other reagents were obtained from commercial suppliers and used without further purification. All the NMR data were recorded on either a Varian Gemini 400 MHz NMR, a Bruker Cryomagnet 400 MHz, or a Bruker UltraShield Magnet 400 MHz, (400 for 1H NMR and 100 13C NMR). Proton experiments are reported in parts per million, ppm) downfield of the signal for tetramethylsilane (TMS). All ^{13}C spectra are reported in ppm relative to the signal for residual chloroform (77 ppm) or methanol (49 ppm). Analytical LC-MS was performed on a C4, Jupiter SuC4300A, 150 × 2.00 mm column with a gradient 5%−100% acetonitrile in H_2O supplemented with 0.1% v/v formic acid (FA) in 15 min. Silica column chromatography was performed manually using silica with particle size 60−200 μm. The purity and exact mass of the compounds were determined using a High Resolution LC-MS system consisting of a Waters ACQUITY UPLC I-Class system coupled to a Xevo G2 quadrupole time of flight (Q-tof) system. The system comprised a Binary Solvent Manager and a Sample Manager with Fixed-Loop (SM-FL). compounds were separated (0.3 mL min−1) on the column (Polaris C18A reverse phase column 2.0 × 100 mm, Agilent) using a 15%−75% acetonitrile gradient in water supplemented with 0.1% v/v FA before analysis in positive mode in the mass spectrometer. On the basis of LC-UV data, all synthesized FC analogs were prepared to ≥95% purity.

Protein expression

His6-tagged 14-3-3σ protein full-length was expressed in NiCo21(DE3) competent cells with a pPROEX HTb plasmid (0.4 mM IPTG, overnight at 18°C), and purified using Ni^{2+}-affinity chromatography. The proteins were dialyzed against FP-buffer (10 mM HEPES pH 7.4, 150mM NaCl) before usage.

Peptide synthesis

Peptides were synthesized via Fmoc solid-phase peptide synthesis (SPPS) using an automated Intavis MultiPep RSi peptide synthesizer. TentaGel R RAM resin (Rapp Polymere; 0.18 mmol/g loading) was used for the synthesis of all peptides. Fmoc-protected amino acid building blocks (Novabiochem®) were dissolved in *N*-methylpyrrolidone (NMP) and coupled sequentially by double coupling to the resin using *N*,*N*-diisopropylethylamine(DIPEA)/(2-(1H-benzotriazol-1-yl)-1,1,3,3-tetramethyluronium hexafluorophos-phate) (HBTU) (4:1 v/v). Fmoc-deprotection was achieved using 20% piperidine in NMP. The peptides were labeled with FITC (Sigma-Aldrich) attached via a short polyethylene glycol-based linker introduced via Fmoc-O1Pen-OH (Iris Biotech) or hexanoic acid-based linker via Fmoc-Ahx-OH (Iris Biotech) following reported procedures.[6] Resin cleavage of the protected peptide was performed using 2.5%/2.5%/95% H_2O/triisopropylsilane (TIS)/trifluoroacetic acid (TFA) and the peptides were subsequently precipitated in ice-cold diethylether. The resultant crude solid was then re-dissolved in acetonitrile/water/0.1%TFA and lyophilized.

The peptides were further purified using a preparative reversed-phase high performance liquid chromatography (HPLC) system which comprised of a LCQ Deca XP Max (Thermo Finnigan) ion-trap mass spectrometer equipped with a Surveyor autosampler and Surveyor photodiode detector array (PDA) detector (Thermo Finnigan). Solvents were pumped using a high-pressure gradient system using two LC-8A pumps (Shimadzu) for the preparative system and a two LC-20AD pumps (Shimadzu) for the analytical system. The crude mixture was purified on a reverse-phase C18 column (Atlantis T3 prep OBD, 5 μm, 150 x 19 mm, Waters) using a flow of 20 mL/min and linear acetonitrile gradient in water with 0.1% v/v trifluoracetic acid (TFA). Fractions with the correct mass were collected using a PrepFC fraction collector (Gilson Inc).

The purity was established by analytical reversed-phase HPLC-MS using a Shimadzu HPLC on a Atlantis® T3 C18 analytical column (2.1x150 mm) LCQ Fleet from Thermo Scientific, Surveyor AS and PDA with an eluent flow rate of 0.2 mL/min (MeCN/H_2O/0.1%TFA) 0-1 min, isocratic, 5% acetonitrile (MeCN); 1-10 min, linear gradient, 5-70%; 10-11 min, isocratic, 70%; 11- 12 min, linear gradient, 70-5%; 12-15 min, isocratic, 5% MeCN. The mass off all peptides corresponded with the calculated mass, with a purity >90%, as determined via the UV-trace.

The p53-peptide (TAMRA-Ahx-SRAHSSHLKSKKGQSTSRHKKLMFK(pT)EGPDSD-*COOH*) was obtained via Anaspec.[7] (Ahx = 6-amino-hexanoic acid)

Fluorescence polarization measurements

Fluorescence anisotropy affinity measurements were conducted in FP-buffer (10 mM HEPES pH 7.4, 150 mM NaCl) with 0.01% TWEEN-20 and 1.0 mg/mL BSA, using fixed concentrations of fluorescently-labeled peptide (10 nM) and DMSO (2% v/v) in 10 µL round-bottom low binding 384-micro well plates (Corning, #25916024). Measurements were performed in triplicate at 20 °C with a filter-based microplate reader (Tecan Infinite F500) using a fluorescein filterset (λ_{ex}:485 nm/20 nm, λ_{em}:535 nm/25 nm), a TAMRA filterset (λ_{ex}:535 nm/25 nm, λ_{em}:595 nm/20 nm) and an integration time of 50 µs, errors bars indicate the standard deviations. The data was fitted using GraphPad Prism 5.05 for Windows (GraphPad Software Inc., CA, USA four-parameter logistic model (4PL) to obtain the EC_{50}-values according to precedent liteature[8,9] and subsequently analyzed with the mathematical model described below.

Semi-synthesis of fusicoccin analogues

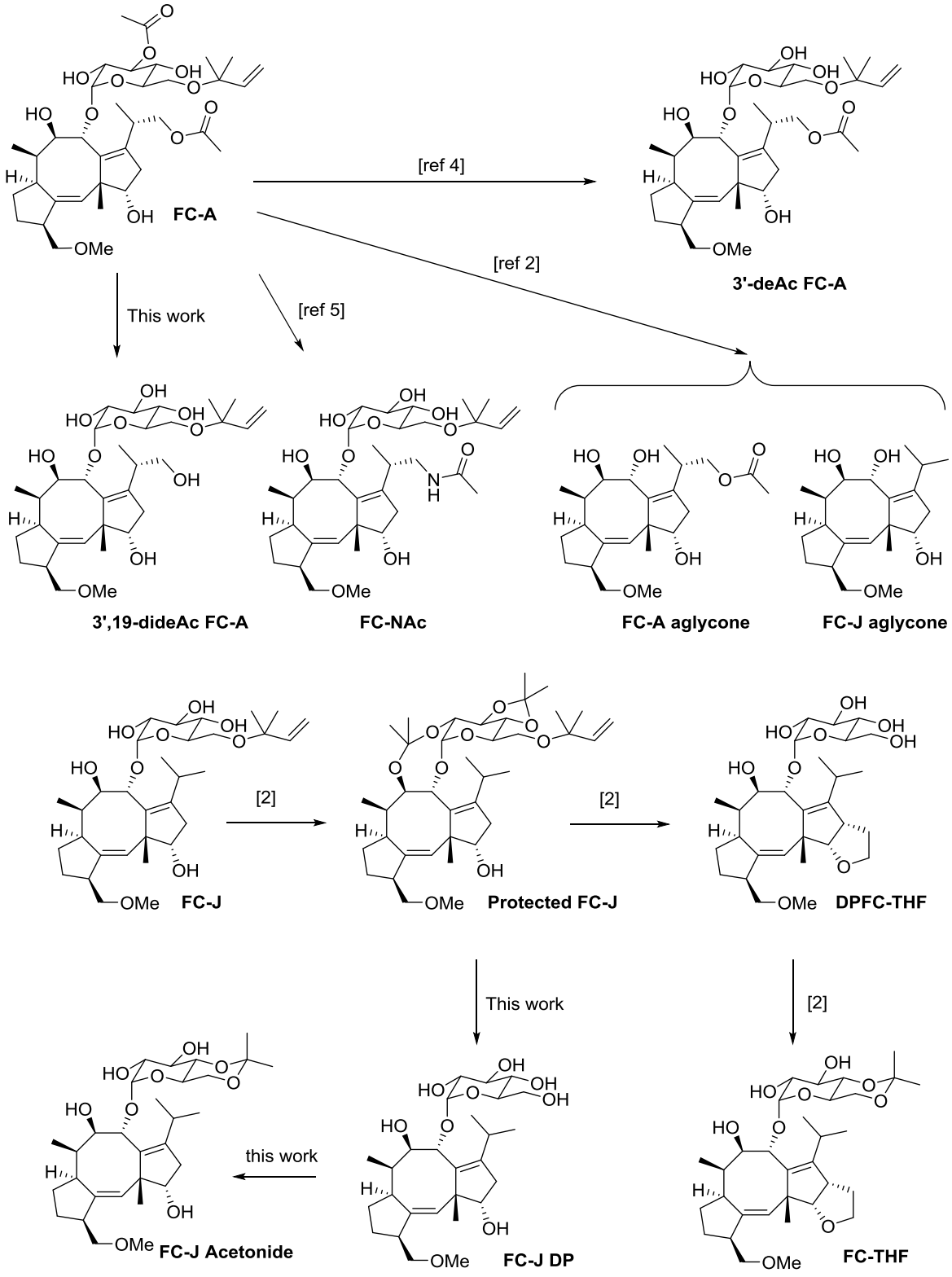

Supporting Figure 4. Overview of synthesis of fusicoccin analogues from FC-A and FC-J.

Synthesis of FC-A 3'-deAc

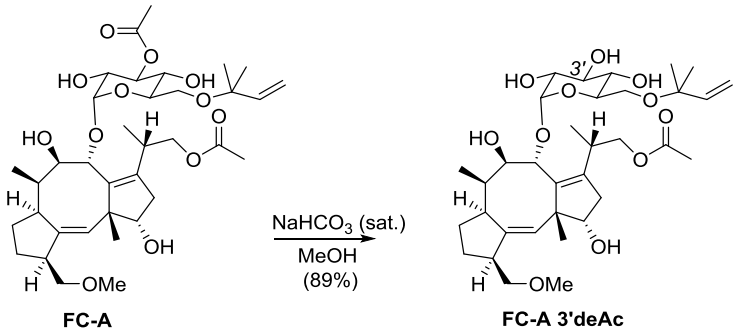

To a solution of FC-A (180 mg, 0.27 mmol) in MeOH (25.0 mL) was added sat. $NaHCO_3$ (30 mL). After stirring at room temperature (rt) for 30 min, the solution was diluted with EtOAc and poured into sat. $KHSO_4$. The organic layer was separated, and the aqueous layer extracted with EtOAc. The combined organic layers were washed with brine and dried over sodium sulfate. After filtration, the solvent was removed *in vacuo*. The residue was purified by flash column chromatography on silica gel to yield FC-A 3′-deAc as a colorless solid (150 mg, 0.24 mmol, 89%). **LC-MS**: $[M+Na]^+$ calculated: 661.36, observed: 661.58. **HRMS**: $[M+Na]^+$ calculated: 661.3564, observed: 661.3553. **^{1}H NMR** (400 MHz, $CDCl_3$-d) δ 5.85 – 5.73 (m, 1H), 5.32 (t, *J* = 2.0 Hz, 1H), 5.15 (dd, *J* = 1.9, 1.2 Hz, 1H), 5.12 (dd, *J* = 5.8, 1.1 Hz, 1H), 5.05 (d, *J* = 3.8 Hz, 1H), 4.28 (dd, *J* = 10.5, 4.8 Hz, 1H), 3.94 (dd, *J* = 10.1, 4.3 Hz, 1H), 3.88 (d, *J* = 10.1 Hz, 1H), 3.85 – 3.75 (m, 3H), 3.69 – 3.59 (m, 2H), 3.53 – 3.45 (m, 2H), 3.45 – 3.38 (m, 3H), 3.36 (s, 3H), 3.36 – 3.30 (m, 1H), 2.89 – 2.68 (m, 2H), 2.40 (dd, *J* = 15.9, 5.8 Hz, 1H), 2.21 (dd, *J* = 15.9, 4.5 Hz, 1H), 2.11 (s, 3H), 2.08 – 1.98 (m, 1H), 1.98 – 1.87 (m, 1H), 1.77 – 1.66 (m, 1H), 1.60 – 1.51 (m, 2H), 1.27 (d, *J* = 2.2 Hz, 6H), 1.20 (s, 3H), 1.10 (d, *J* = 6.8 Hz, 3H), 0.89 (d, *J* = 7.0 Hz, 3H). **^{13}C NMR** (100 MHz, $CDCl_3$) δ 172.06, 148.25, 143.28, 139.96, 139.52, 125.63, 114.69, 100.95, 79.19, 78.41, 76.54, 76.27, 76.05, 73.84, 72.76, 72.29, 70.85, 68.36, 63.46, 58.91, 56.68, 47.82, 41.95, 37.56, 36.27, 32.99, 28.53, 25.98, 25.52, 24.81, 21.33, 15.58, 10.23, 0.15.

Synthesis of FC-A (19,3')dideAc

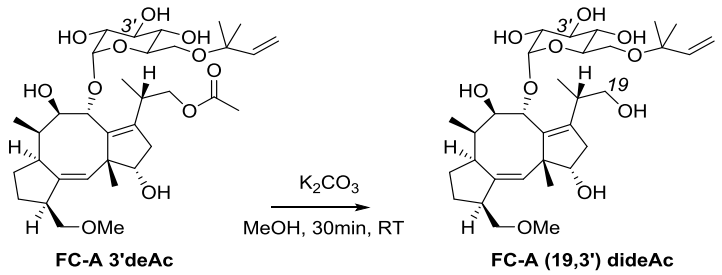

To a solution of FC-A (100 mg, 0.15 mmol) in 1.36 mL MeOH was 43.3mg. K_2CO_3. After stirring at room temperature (rt) for 30 min, the solution was acidified 10% citric acid and extracted with chloroform. The combined organic layers were washed with brine and dried over sodium sulfate. After filtration, the solvent was removed *in vacuo*. The residue was purified by flash column chromatography on silica gel to yield FC-A (19,3′)-dideAc as a colorless solid, 96 mg (0.142 mmol, 95%). **LC-MS**: $[M+Na]^+$ calculated: 619.35, observed: 619.58. **HRMS**: $[M+Na]^+$ calculated: 619.3458, observed: 619.3464. **^{1}H NMR** (400 MHz, $CDCl_3$) δ 5.91 – 5.70 (m, 1H), 5.50 (s, 1H), 5.33 (t, *J* = 1.9 Hz, 1H), 5.19 – 5.12 (m, 1H), 5.11 (dd, *J* = 5.2, 1.1 Hz, 1H), 5.04 (d, *J* = 3.8 Hz, 1H), 4.67 (s, 1H), 4.45 (s, 1H), 4.37 (s, 1H), 3.98 (dd, *J* = 10.1, 4.4 Hz, 1H), 3.89 (d, *J* = 10.0 Hz, 1H), 3.84 – 3.71 (m, 2H), 3.66 – 3.54 (m, 3H), 3.52 – 3.37 (m, 6H), 3.36 (s, 3H), 3.28 – 3.13 (m, 1H), 2.91 – 2.69 (m, 2H), 2.34 (dd, *J* = 15.8, 5.9 Hz, 1H), 2.17 (dd, *J* = 15.8, 4.7 Hz, 1H), 2.04 – 1.91 (m, 2H), 1.74 – 1.65 (m, 1H), 1.64 – 1.48 (m, 2H), 1.27 (s, 3H), 1.27 (s, 3H), 1.18 (s, 3H), 1.08 (d, *J* = 6.6 Hz, 3H), 0.87 (d, *J* = 7.0 Hz, 3H). **^{13}C NMR** (100 MHz, $CDCl_3$) δ 147.71, 143.38, 141.05, 139.05, 125.88, 114.66, 100.95, 79.41, 78.62, 76.23, 76.11, 75.92, 73.48, 72.02, 71.97, 71.04, 66.64, 63.17, 58.88, 56.31, 47.88, 41.90, 41.64, 37.29, 36.38, 36.36, 28.45, 25.93, 25.54, 24.76, 15.25, 10.09, 0.15.

Synthesis of FC-J DP

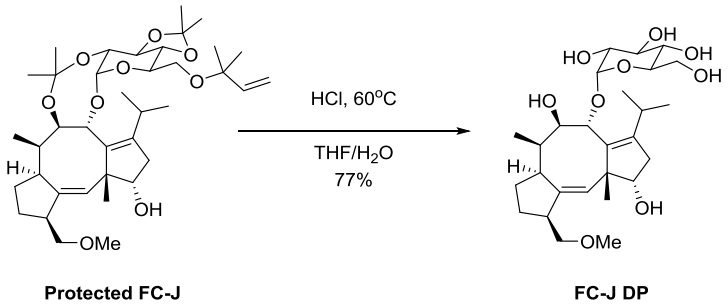

FC-J (440 mg, 0.666 mmol) was dissolved in 10 mL methanol and heated to 60 °C. To the solution was added 3.5 mL 2.0 M HCl aqueous solution and the reaction stirred for 6 h. After cooling down, the reaction was quenched with 1 mL NEt_3, the solvent evaporated and the crude product purified by silica gel chromatography (DCM/acetone/MeOH 100/50/17 v/v/v) yielding a colorless oil. The oil was dissolved in MilliQ water and lyophilized yielding 263 mg (0.51 mmol, 77%) of FC-J DP as a white amorphous powder. **LC-MS**: $[M+Na]^+$ expected: 535.29, observed: 535.50. **HRMS**: $[M+H]^+$ calculated: 513.3064, observed: 513.3060 **H NMR**: (400 MHz, CD_3OD) δ 5.40 (t, *J* = 1.8 Hz, 1H), 4.92 (d, *J* = 3.8 Hz, 1H), 3.96 (dd, *J* = 10.1, 4.2 Hz, 1H), 3.83 (d, *J* = 10.0 Hz, 1H), 3.78 – 3.58 (m, 5H), 3.45 – 3.41 (m, 1H), 3.41 – 3.35 (m, 1H), 3.33 (s, 3H), 3.34 – 3.29 (m, 2H), 3.27 – 3.17 (m, 1H), 2.93 – 2.67 (m, 2H), 2.32 (dd, *J* = 14.4, 6.8 Hz, 1H), 2.01 – 1.87 (m, 3H), 1.66 – 1.43 (m, 3H), 1.21 (s, 3H), 1.08 (d, *J* = 6.6 Hz, 3H), 0.96 (d, *J* = 6.8 Hz, 3H), 0.83 (d, *J* = 7.2 Hz, 3H). **^{13}C NMR**: (100 MHz, CD_3OD) δ 146.65, 142.57, 136.29, 128.26, 103.79, 82.99, 79.90, 79.18, 77.14, 75.04, 73.91, 73.74, 71.27, 62.19, 58.83, 54.24, 49.91, 43.04, 42.64, 36.72, 35.52, 29.24, 28.34, 24.20, 21.82, 20.74, 9.91.

Synthesis of FC-J Acetonide

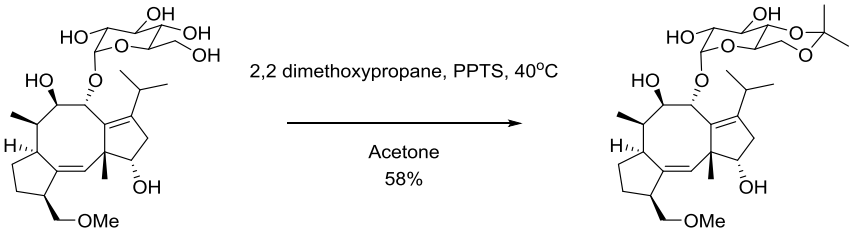

FC-J DP (163 mg, 0.318 mmol) was dried by azeotropical distillation from 2 x 20 mL toluene/EtOH 8/1 v/v and 1 x 20 mL toluene. The dried flask was back-filled with argon and the material dissolved in 10 mL anhydrous acetone (overnight drying in $CaSO_4$). To the solution were added 125 µL 2,2-dimethoxypropane and 5 mg pyridinium paratoluenesulfonate (PPTS) and the temperature was raised to 40 °C. After stirring overnight, an additional 50 µL 2,2-dimethoxypropane was added and again after an additional 6 h. After stirring for 1 h after the last addition, the reaction mixture was diluted in Et_2O and poured into brine. The mixture was extracted with Et_2O thrice, dried over $MgSO_4$, filtered and the solvent evaporated. The crude was purified by silica gel column chromatography (DCM/acetone/MeOH 100/20/5 v/v/v) yielding a clear oil. The oil was dissolved in MilliQ water and lyophilized yielding 104 mg (0.184 mmol, 58%) FC-J acetonide as a white amorphous powder. **LC-MS**: $[M+Na]^+$ expected: 575.32, observed: 575.58. **HRMS**: $[M+H]^+$ calculated: 553.3377, observed: 553.3372 **^{1}H NMR**: (400 MHz, Methanol-d4) δ 5.40 (t, *J* = 1.9 Hz, 1H), 4.89 (d, *J* = 3.8 Hz, 1H), 3.96 (dd, *J* = 10.0, 4.2 Hz, 1H), 3.79 (d, *J* = 10.0 Hz, 1H), 3.77 – 3.61 (m, 5H), 3.49 (dd, *J* = 9.4, 3.6 Hz, 1H), 3.47 – 3.42 (m, 1H), 3.33 (s, 3H), 3.30 – 3.28 (m, 2H), 3.28 – 3.22 (m, 1H), 2.92 – 2.67 (m, 2H), 2.36 (dd, *J* = 14.4, 6.7 Hz, 1H), 2.09 – 1.84 (m, 3H), 1.63 – 1.50 (m, 3H), 1.47 (s, 3H), 1.33 (s, 3H), 1.16 (s, 3H), 1.13 (d, *J* = 6.6 Hz, 3H), 0.99 (d, *J* = 6.8 Hz, 3H), 0.83 (d, *J* = 7.2 Hz, 3H). **^{13}C NMR**: (100 MHz, CD_3OD δ 146.78, 142.74, 136.25, 128.08, 104.21, 100.80, 83.14, 79.67, 79.28, 77.12, 75.47, 74.39, 72.36, 65.29, 63.60, 58.83, 54.38, 49.90, 42.98, 42.57, 36.72, 35.50, 29.52, 29.15, 28.36, 24.22, 21.55, 20.93, 19.30, 9.92.

Mathematical Model

Derivation and numerical solution

Supporting Figure 4 depicts the scheme of equilibria involved in protein-protein interaction stabilization via sequential addition of model peptide and stabilizer to a receptor protein via pathway A or pathway B, stabilizer and peptide respectively. The peptide-ligand binds to a receptor with K_D^I, in the presence of a stabilizer, this affinity is altered to K_D^{III}. Similarly, the stabilizer binds with an intrinsic affinity K_D^{II} and an enhanced affinity K_D^{IV} when the peptide is already bound.

Definition of terms:

R_{tot} : total concentration of 14-3-3 monomer
P_{tot}: total concentration of labeled partner
S_{tot}: total concentration of stabilizer compound

K_D^I: dissociation equilibrium constant for the binding of the partner to 14-3-3 monomer
K_D^{II}: dissociation equilibrium constant for the binding of the stabilizer to 14-3-3 monomer
K_D^{III}: dissociation equilibrium constant for the binding of the partner to 14-3-3 monomer in complex with stabilizer
K_D^{IV}: dissociation equilibrium constant for the binding of the stabilizer to 14-3-3 monomer in complex with stabilizer the partner

α: cooperativity factor

[R]: free concentration 14-3-3
[P]: free concentration labeled partner
[S]: free concentration stabilizer

[R•P]: concentration 14-3-3/partner complex
[R•S]: concentration 14-3-3/stabilizer complex
[R•S•P]: concentration 14-3-3/partner/stabilizer complex

With the exception of α, which is dimensionless, the unit of all terms is expressed in $mol \cdot L^{-1}$.

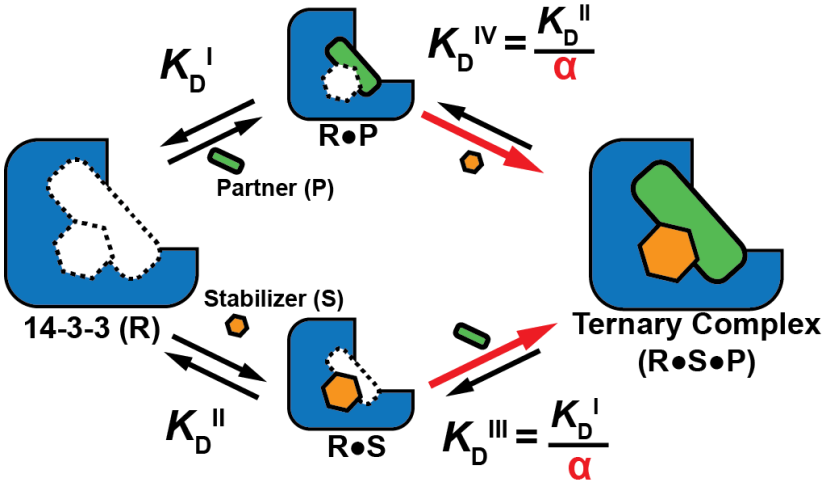

Supporting Figure 5. Schematic representation of the various equilibria involved in PPI stabilization as depicted in the main manuscript Figure 3.

The mass-balances of the total concentration of receptor protein, stabilizer and labeled partner species are first partitioned between their respective free forms and various complexes (Eq. 1–3).

$$R_{tot} = [R] + [R{\bullet}P] + [R{\bullet}S] + [R{\bullet}S{\bullet}P] \quad (1)$$

$$S_{tot} = [S] + [R{\bullet}S] + [R{\bullet}S{\bullet}P] \quad (2)$$

$$P_{tot} = [P] + [R{\bullet}P] + [R{\bullet}S{\bullet}P] \quad (3)$$

Next, the equilibrium equations of the dissociation constant K_Ds, and its related species are expressed. (Eq. 4–7).

$$K_D^I = \frac{[R] \times [P]}{[R{\bullet}P]} \quad (4)$$

$$K_D^{II} = \frac{[R] \times [S]}{[R{\bullet}S]} \quad (5)$$

$$K_D^{III} = \frac{[R{\bullet}S] \times [P]}{[R{\bullet}S{\bullet}P]} \quad (6)$$

$$K_D^{IV} = \frac{[R{\bullet}P] \times [S]}{[R{\bullet}S{\bullet}P]} \quad (7)$$

The cooperativity constant α is defined as the ratio of non-stabilized and stabilized binding:

$$\alpha = \frac{K_D^I}{K_D^{III}} = \frac{K_D^{II}}{K_D^{IV}} \quad (8)$$

The equilibrium constants are substituted in Eq. 6 & 7:

$$\frac{K_D^I}{\alpha} = \frac{[R{\bullet}S] \times [P]}{[R{\bullet}S{\bullet}\mathrm{P}]} \quad (9)$$

$$\frac{K_D^{II}}{\alpha} = \frac{[R{\bullet}P] \times [S]}{[R{\bullet}S{\bullet}P]} \quad (10)$$

The equilibrium equations are then rewritten to obtain expressions for all complexes [R•P], [R•S], [R•S•P] as a function of the dissociation constants relevant parameters and free concentrations of all species (Eq. 11–13).

$$[R{\bullet}P] = \frac{[R] \times [P]}{K_D^I} \quad (11)$$

$$[R{\bullet}S] = \frac{[R] \times [S]}{K_D^{II}} \quad (12)$$

$$[R{\bullet}\mathrm{S}{\bullet}P] = \frac{[R] \times [S] \times [P] * \alpha}{K_D^I \times K_D^{II}} \quad (13)$$

The equations 11–13 are substituted in the mass-balance equations (Eq. 1-3) to arrive at the following expressions:

$$R_{tot} = [R] + \frac{[R] \times [P]}{K_D^I} + \frac{[R] \times [S]}{K_D^{II}} + \frac{[R] \times [S] \times [P] \times \alpha}{K_D^I \times K_D^{II}} \quad (14)$$

$$S_{tot} = [S] + \frac{[R] \times [S]}{K_D^{II}} + \frac{[R] \times [S] \times [P] \times \alpha}{K_D^I * K_D^{II}} \quad (15)$$

$$P_{tot} = [P] + \frac{[R] \times [P]}{K_D^I} + \frac{[R] \times [S] \times [P] \times \alpha}{K_D^I \times K_D^{II}} \quad (16)$$

Which can be rewritten to gain expressions for R, S and P (Eq. 17-19):

$$[R] = \frac{R_{tot}}{1 + \frac{[P]}{K_D^I} + \frac{[S]}{K_D^{II}} + \frac{[S] \times [P] \times \alpha}{K_D^I \times K_D^{II}}} \quad (17)$$

$$[S] = \frac{S_{tot}}{1 + \frac{[R]}{K_D^{II}} + \frac{[R] \times [P] \times \alpha}{K_D^I \times K_D^{II}}} \quad (18)$$

$$[P] = \frac{P_{tot}}{1 + \frac{[R]}{K_D^I} + \frac{[R] \times [S] \times \alpha}{K_D^I \times K_D^{II}}} \quad (19)$$

Finally, custom-written MATLAB scripts are used to solve the coupled non-linear equations 17-19 for the free concentrations R, P and S through iteration over the three equations. The free concentrations R, P, and S can subsequently be filled in (Eq. 11-13) to calculate the equilibrium concentrations of all other species, most importantly the labeled species P, R•P and R•S•P. Once all the concentrations are calculated, the normalized calculated anisotropy signal (r_{model}) is obtained by (Eq. 20):

$$r_{model} = \frac{P_{tot} - [P]}{P_{tot}} \quad (20)$$

Data analysis and parameter estimation

To determine K_D^{II} and α, we performed non-linear least square analysis on the 2D fluorescence anisotropy assay data as reported in Figures 1, 2, 3 in the main manuscript and Supporting Figure 1. The experimental anisotropy data of all relative concentrations of receptor and stabilizer was compared to the anisotropy values of the modeled titration data.

$$cost = \frac{\sum (r_{model} - r_{experimental})^2}{\#datapoints} \quad (21)$$

Nonlinear least square minimization of the data was performed to minimize the cost function (Eq. 21) using the MATLAB function lsqnonlin, a subspace trust region method based on the interior-reflective Newton method. In order to prevent entrapment in a local minimum, 30 different starting values of K_D^{II}, α were defined, and the best fit (defined as the fit with the lowest square of the norm of the residuals) is taken as the final solution for the optimized values. The different initial parameter sets are defined using a latin hypercube sampling method (MATLAB function lhsdesign)[10].

The MATLAB scripts can be obtain from the authors upon request.

Spectra

LCMS analysis data for the peptides

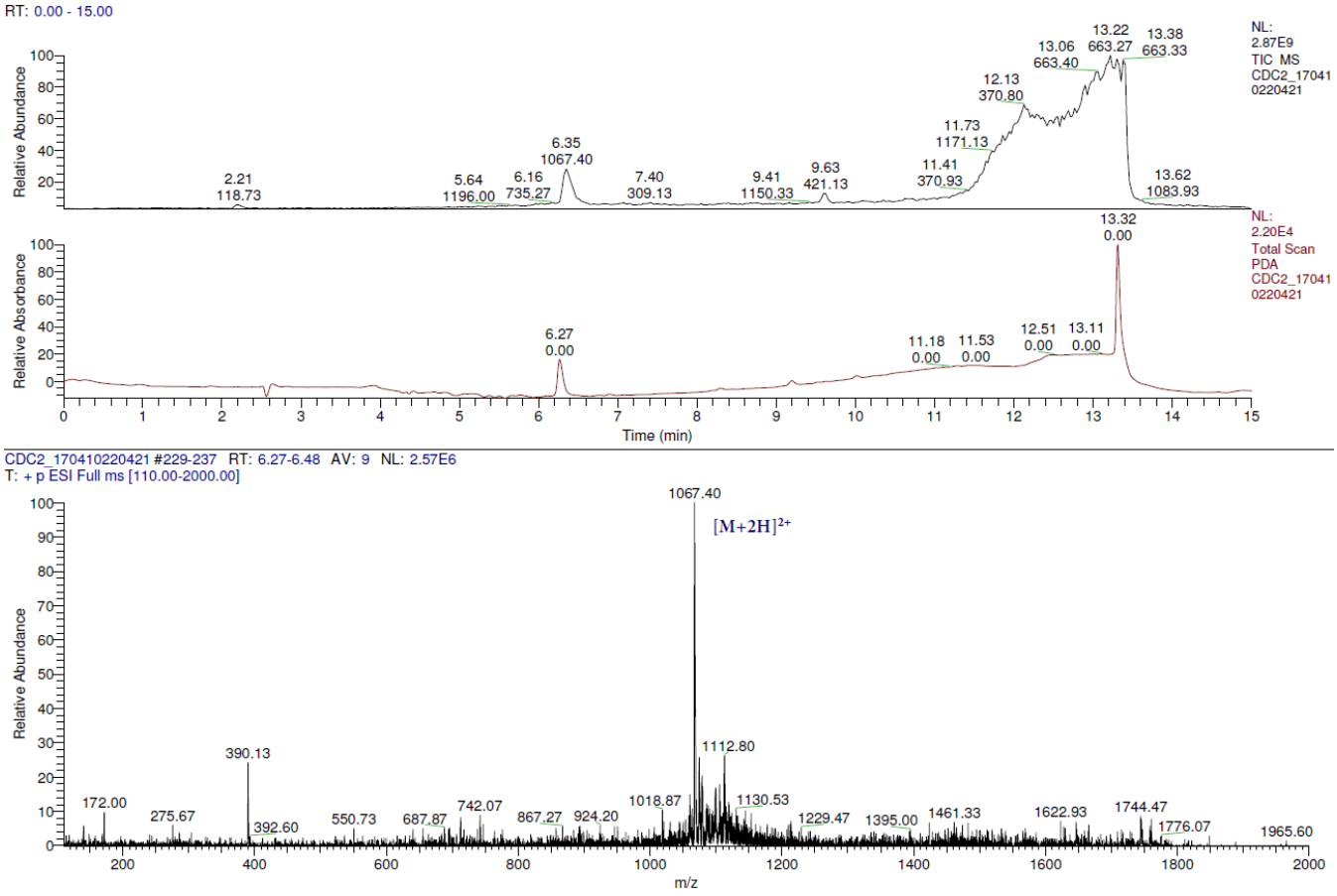

Supporting Figure 6. Analytical data for CDC25C: FITC-O1Pen-SGLYRSP(pS)MPENLN-CONH$_2$, R_t=6.3; ESI-MS: $[M+2H]^{2+}$, calculated 1067,4, observed 1067.4;

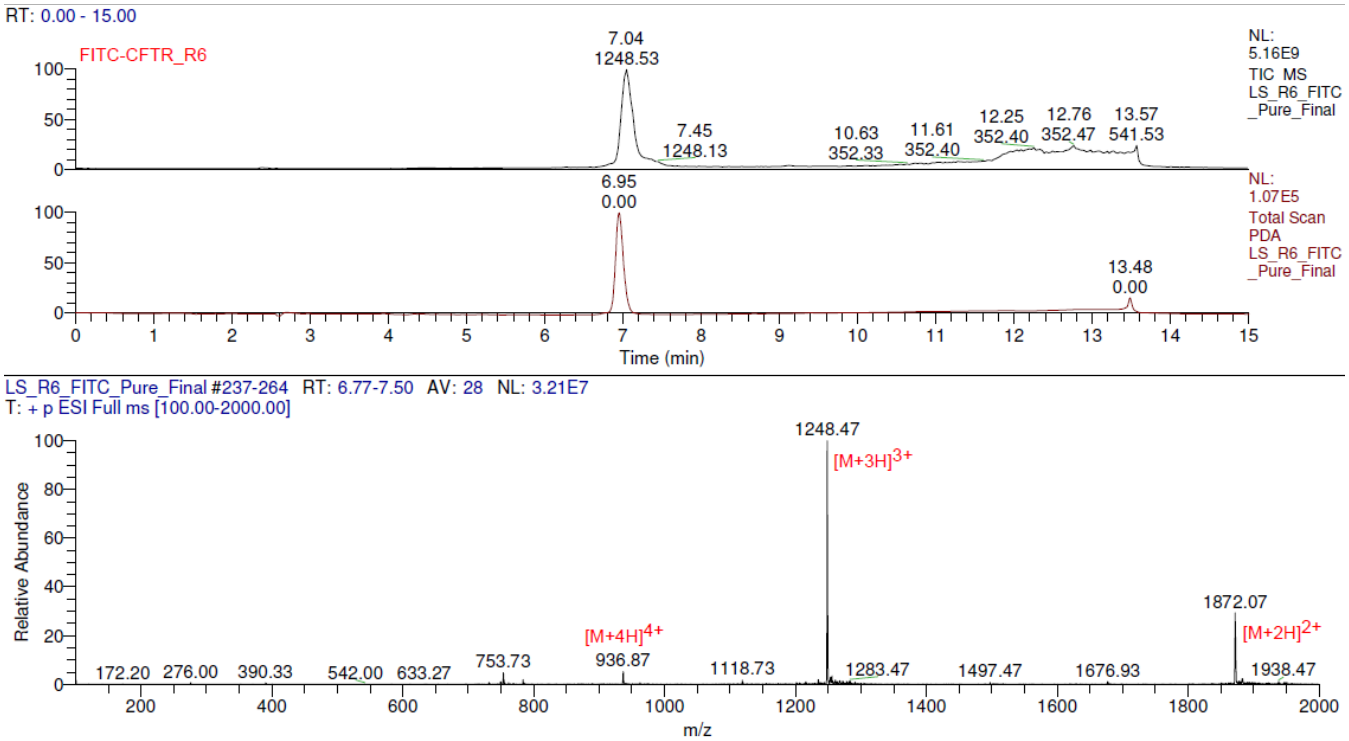

Supporting Figure 7. Analytical data for CFTR: FITC-O1Pen-SQRQRST(pS)TPNVH-$CONH_2$,[1] R_t=7.0; ESI-MS: $[M+2H]^{2+}$, calculated 1870.9, observed 1872.1; $[M+3H]^{3+}$, calculated 1247.6, observed 1248.5; $[M+4H]^{4+}$, calculated 936.0, observed 936.9;

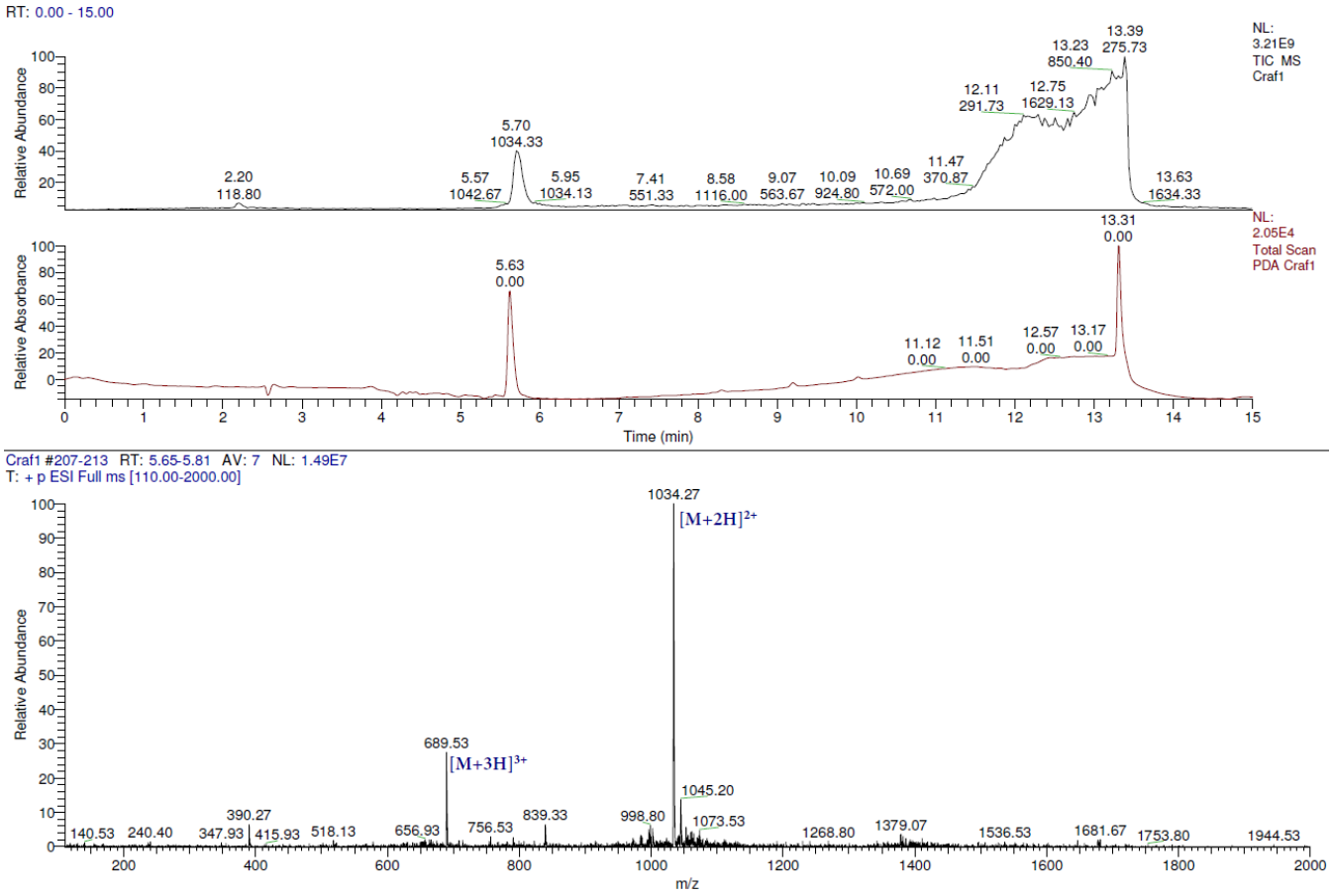

Supporting Figure 8. Analytical data for CRAF: FITC-O1Pen-SQRQRST(pS)TPNVH-CONH$_2$, R_t=5.7; ESI-MS: $[M+2H]^{2+}$, calculated 1033.9, observed 1034.3; $[M+3H]^{3+}$, calculated 689.6, observed 689.5;

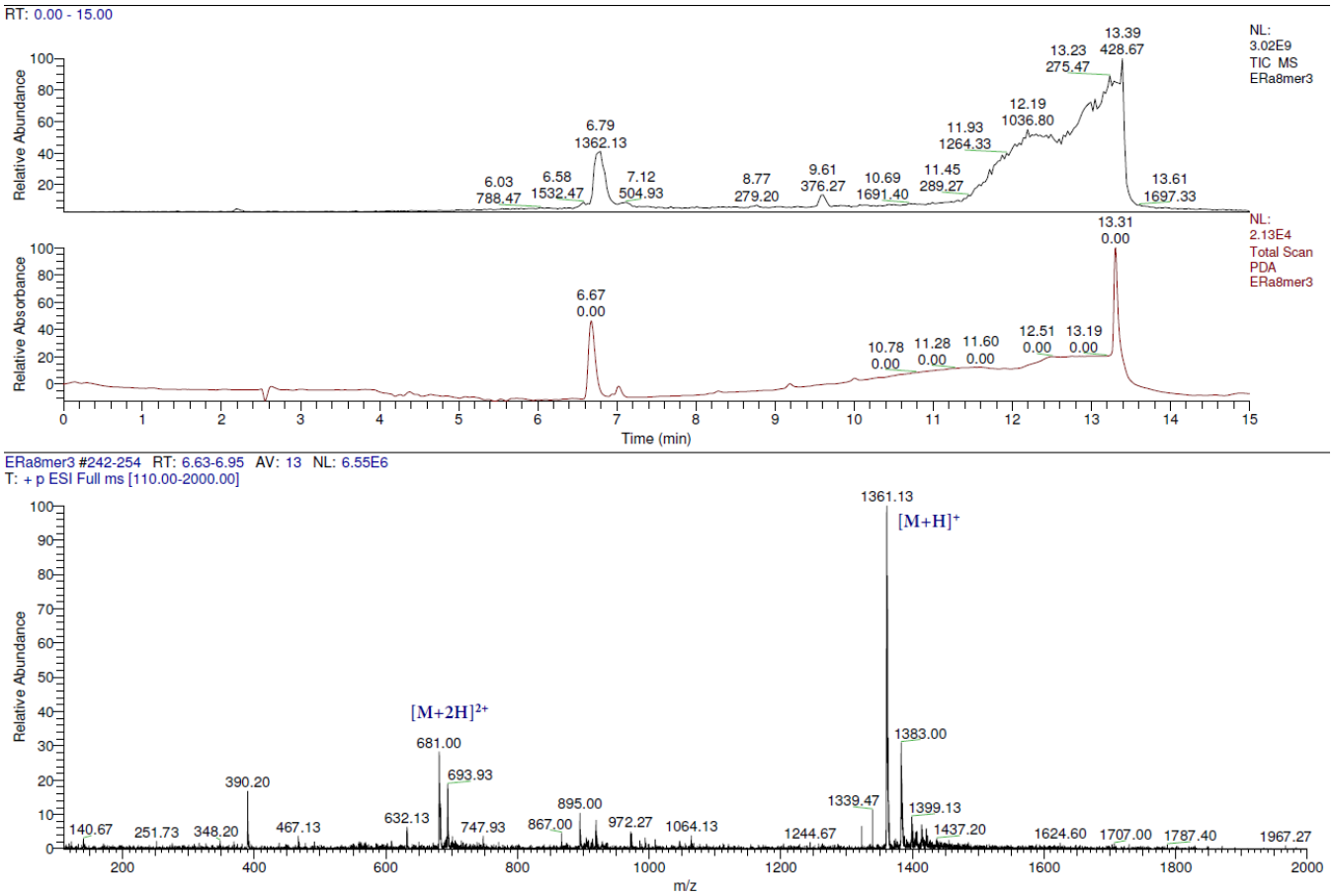

Supporting Figure 9. Analytical data for ERα: FITC-O1Pen-AEGFPA(pT)V-*COOH*,[11] R_t=6.8; ESI-MS: $[M+H]^+$, calculated 1361.5, observed 1361.1; $[M+2H]^{2+}$, calculated 681.3, observed 681.0;

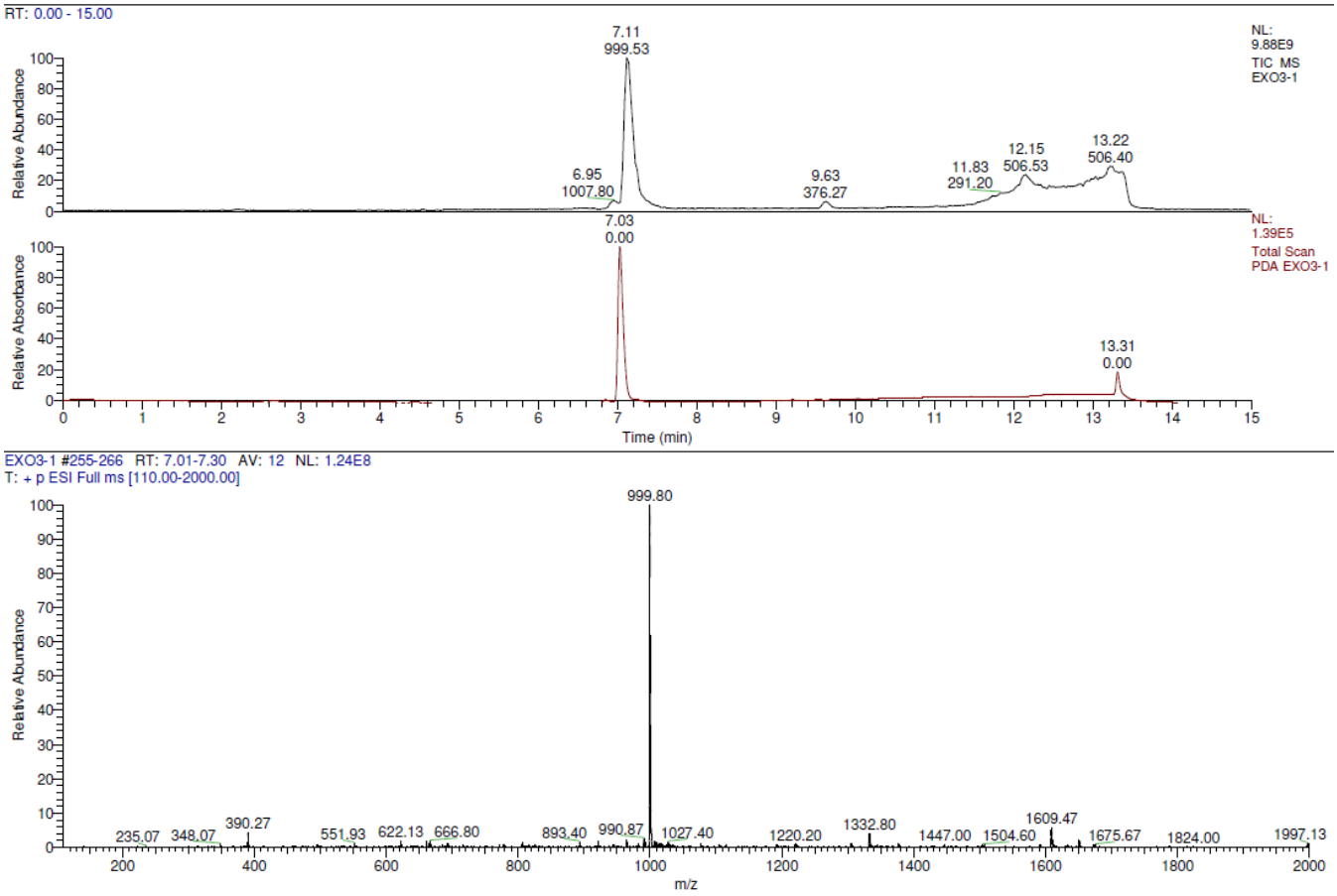

Supporting Figure 10. Analytical data for ExoS: FITC-O1pen-SGHSQGLLDALDAS-$CONH_2$,[3] R_t=6.8; ESI-MS: $[M+2H]^{2+}$, calculated 999.9, observed 999.8;

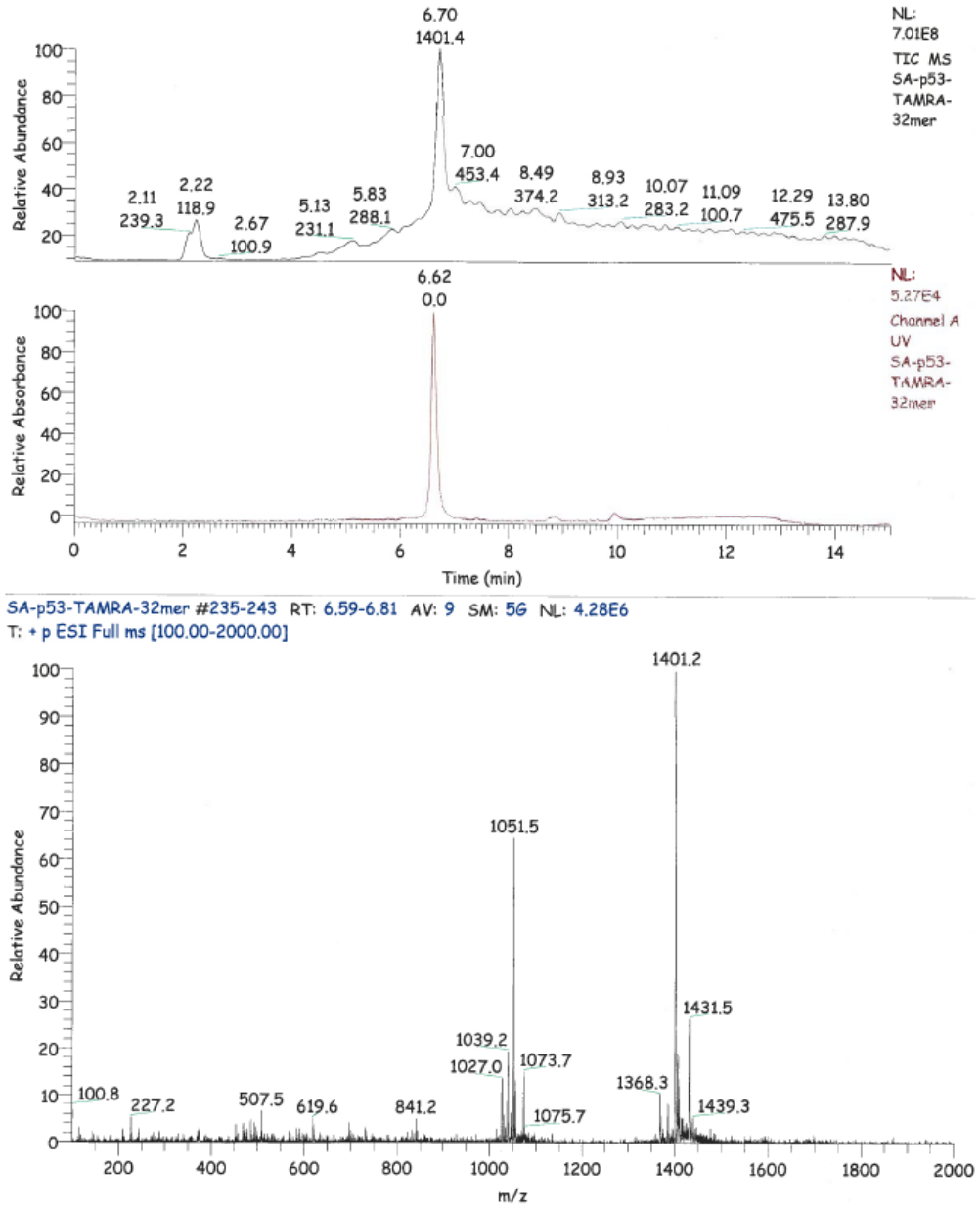

Supporting Figure 11. Analytical data for P53: TAMRA-Ahx-SRAHSSHLKSKKGQSTSRHKKLMFK(pT)EGPDSD-COOH,[7] R_t=6.7; ESI-MS: $[M+3H]^{3+}$, calculated 1401.0 observed 1401.2; $[M+4H]^{4+}$, calculated 1051.0, observed 1051.5;

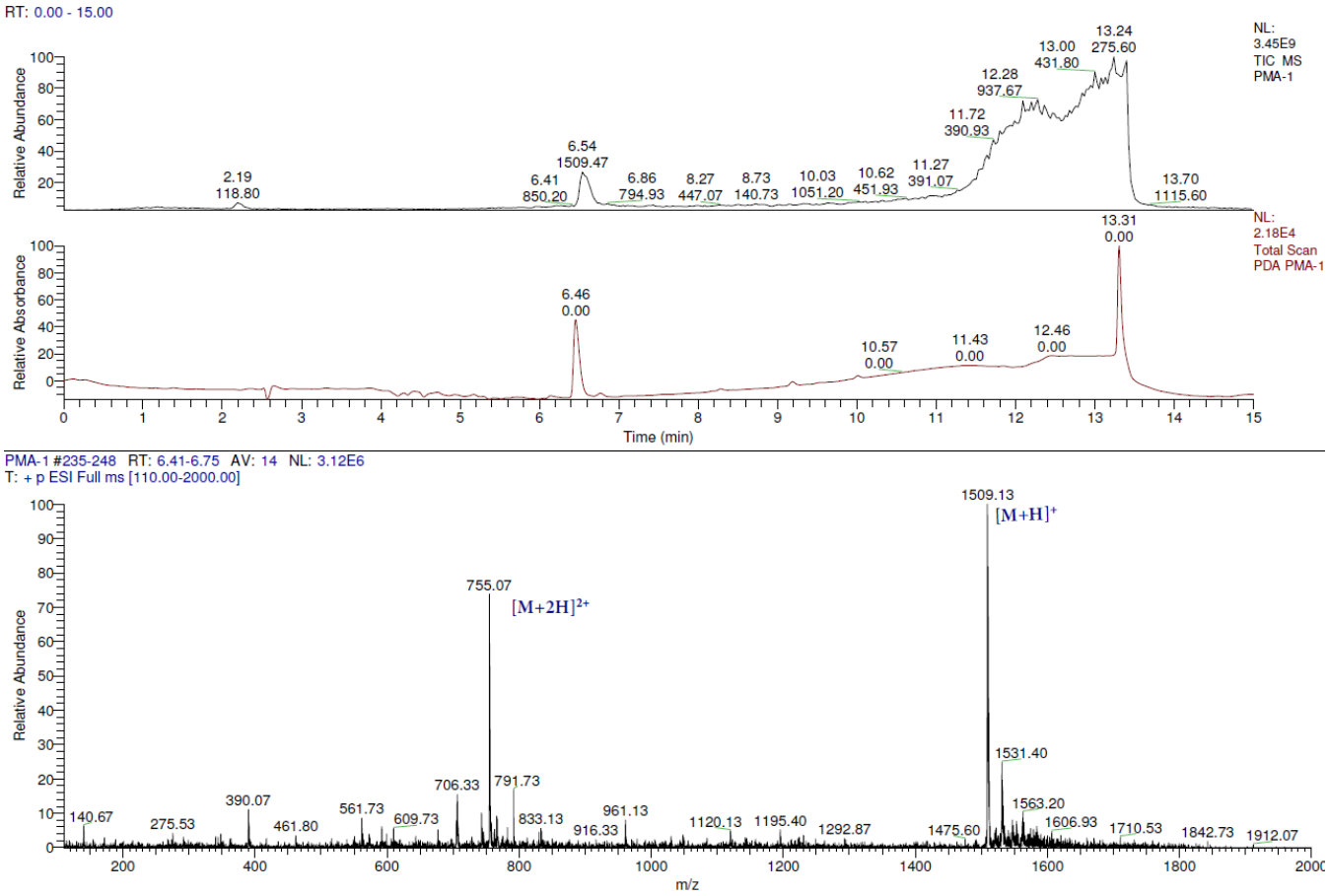

Supporting Figure 12. Analytical data for PMA2: FITC-O1Pen-TIQQSYpTV-COOH,[12] R_t=6.5; ESI-MS: $[M+H]^+$, calculated 1509.6 observed 1509.1; $[M+2H]^{2+}$, calculated 755.3, observed 755.0;

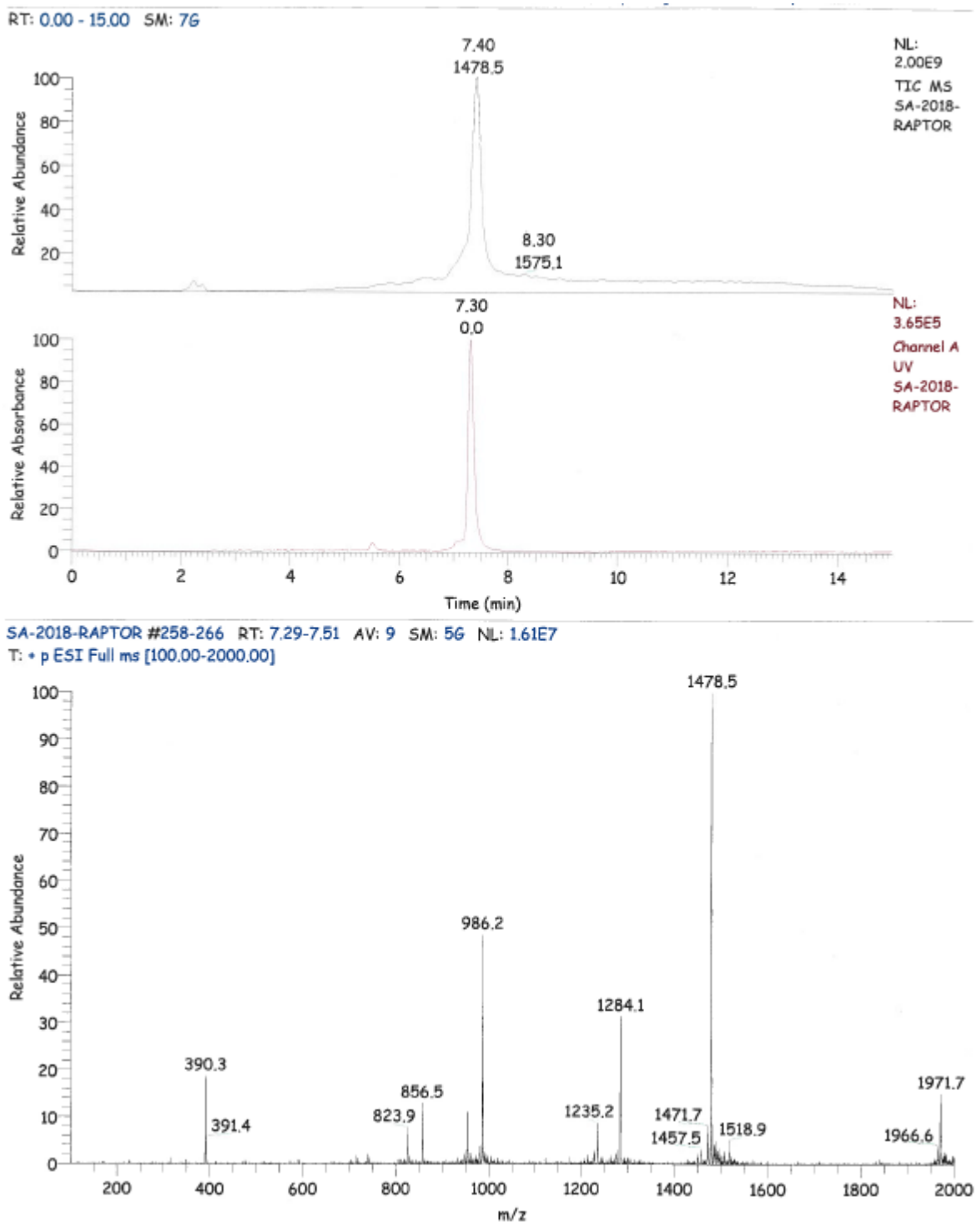

Supporting Figure 13. Analytical data for RAPTOR: FITC - Ahx - GAKDTEWRSV(pT)LPRDLQSTGR-COOH, R_t=7.4; ESI-MS: $[M+2H]^{2+}$, calculated 1478,4 observed 1478,5; $[M+2H]^{2+}$, calculated 985.9, observed 986.2;

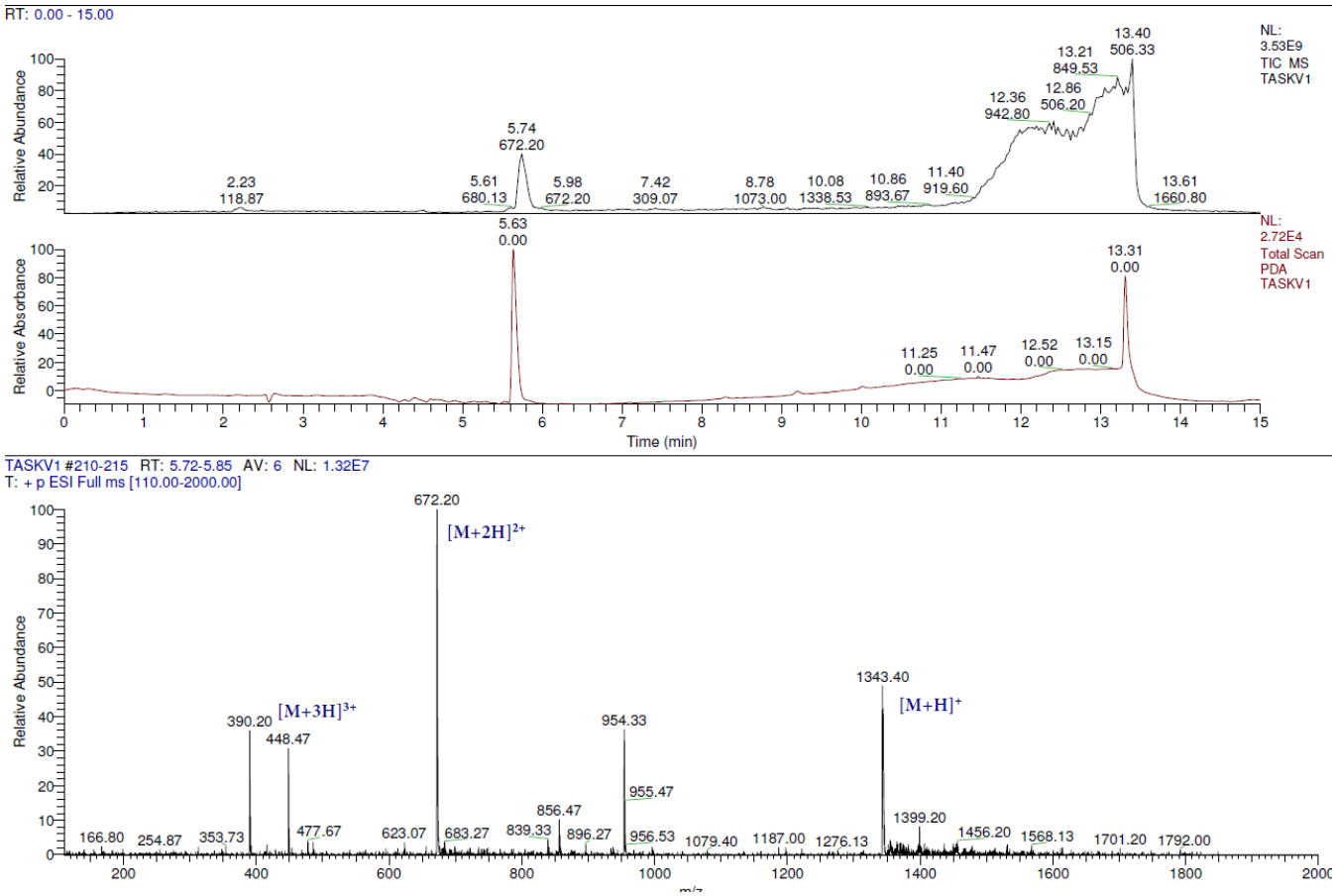

Supporting Figure 14. Analytical data for TASK3: FITC-O1Pen-KRRK(pS)V-*COOH*,[2] R_t =5.7; ESI-MS: $[M+2H]^{2+}$, calculated 1343,6 observed 1343.4; $[M+2H]^{2+}$, calculated 672.3, observed 672.2; $[M+3H]^{3+}$, calculated 448.5, observed 448.5;

NMR Spectra

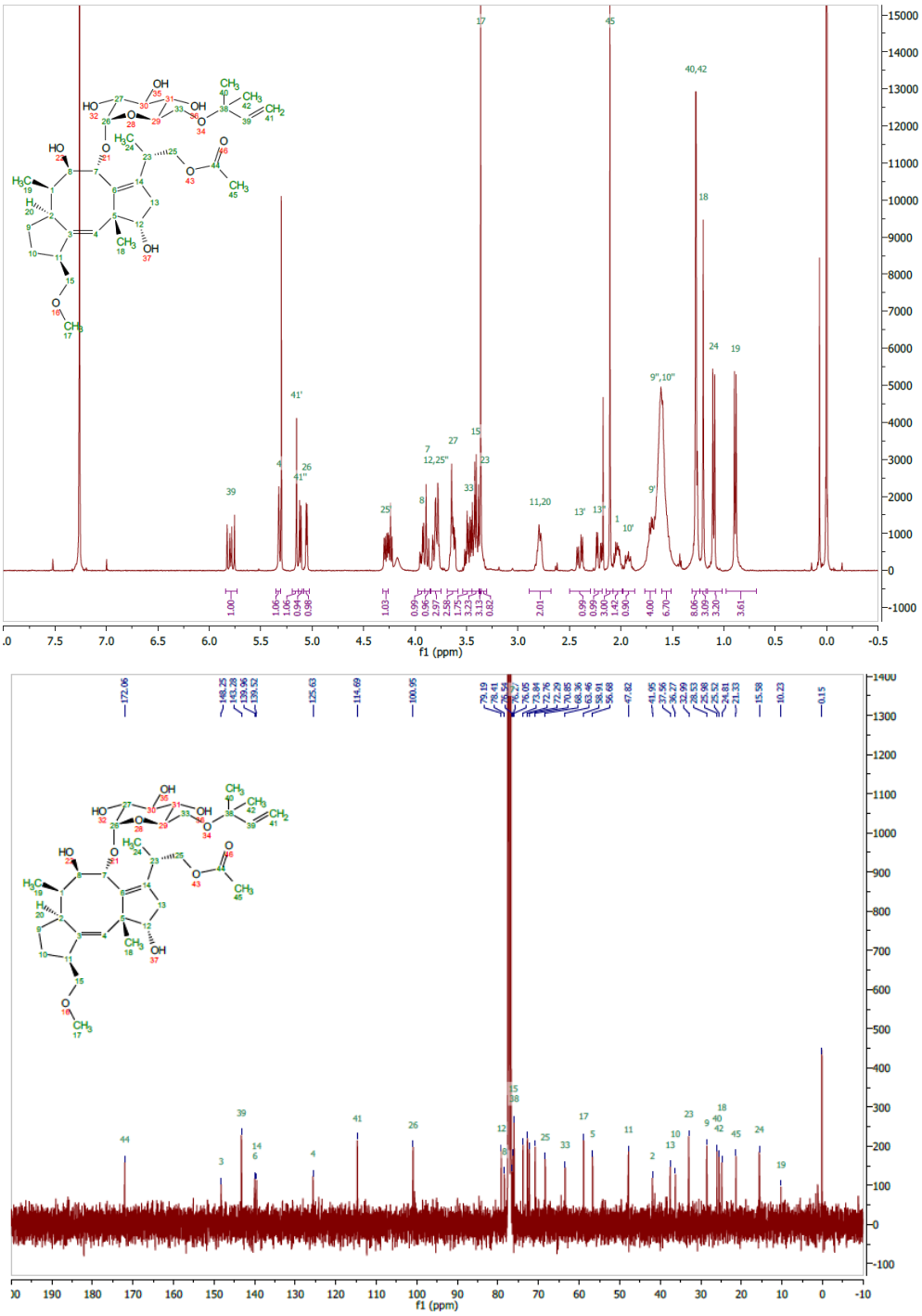

Supporting Figure 15. ^{1}H and ^{13}C NMR spectra of **FC-A 3'-deAc** in $CDCl_3$.

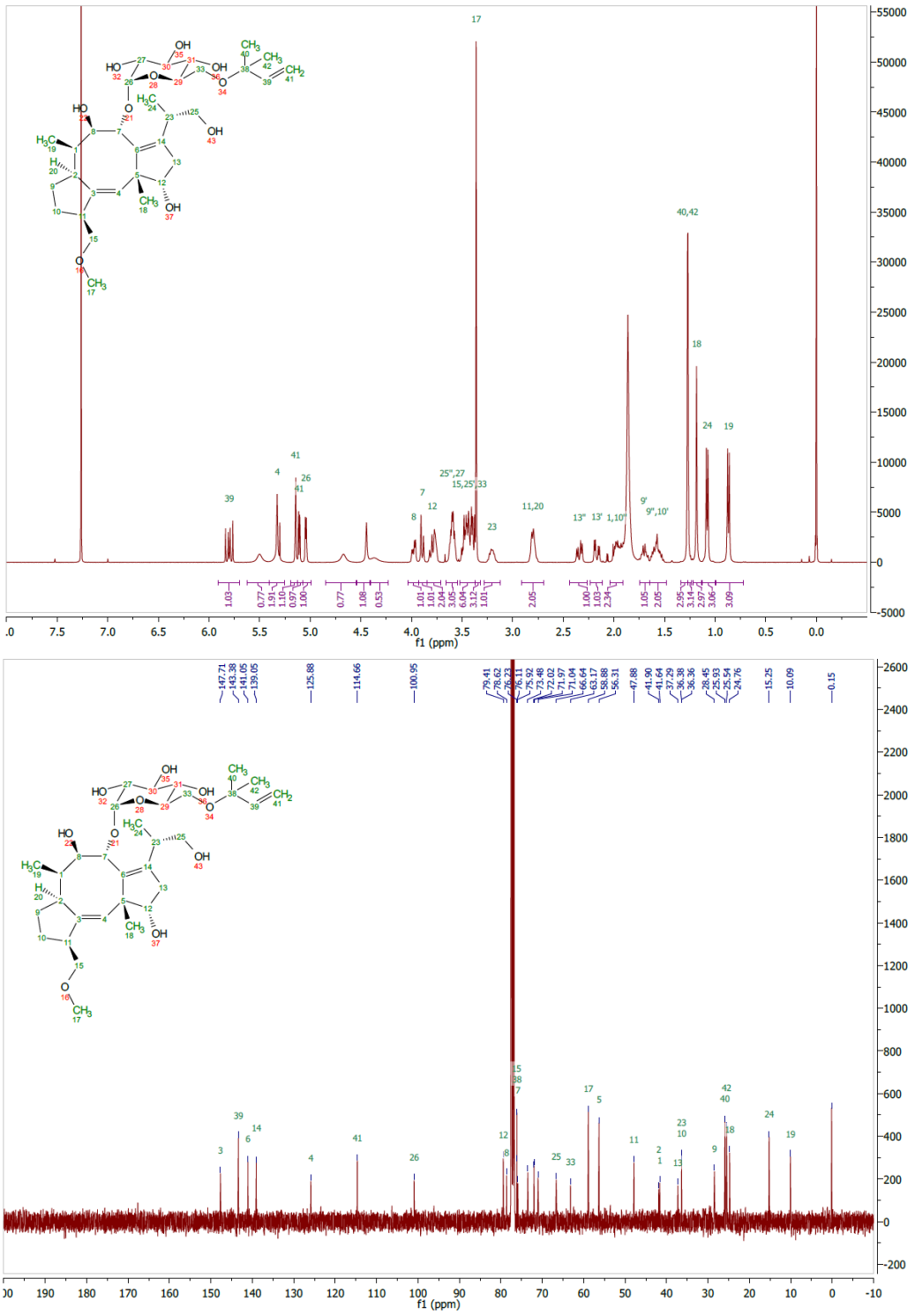

Supporting Figure 16. ^{1}H and ^{13}C NMR spectra of **FC-A 3'-deAc** in $CDCl_3$.

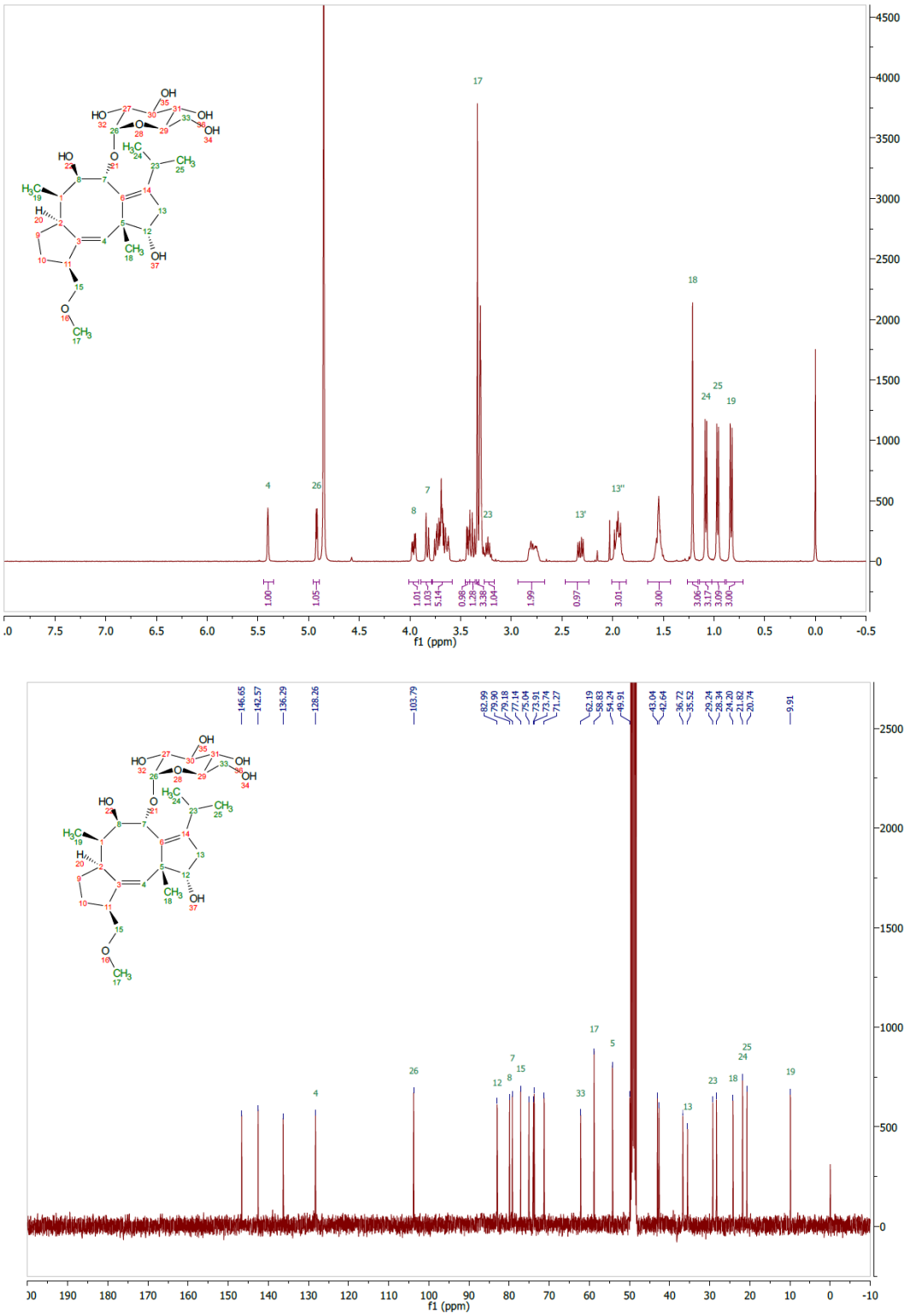

Supporting Figure 17. 1H and 13C NMR spectra of **FC-J DP** in CD_3OD.

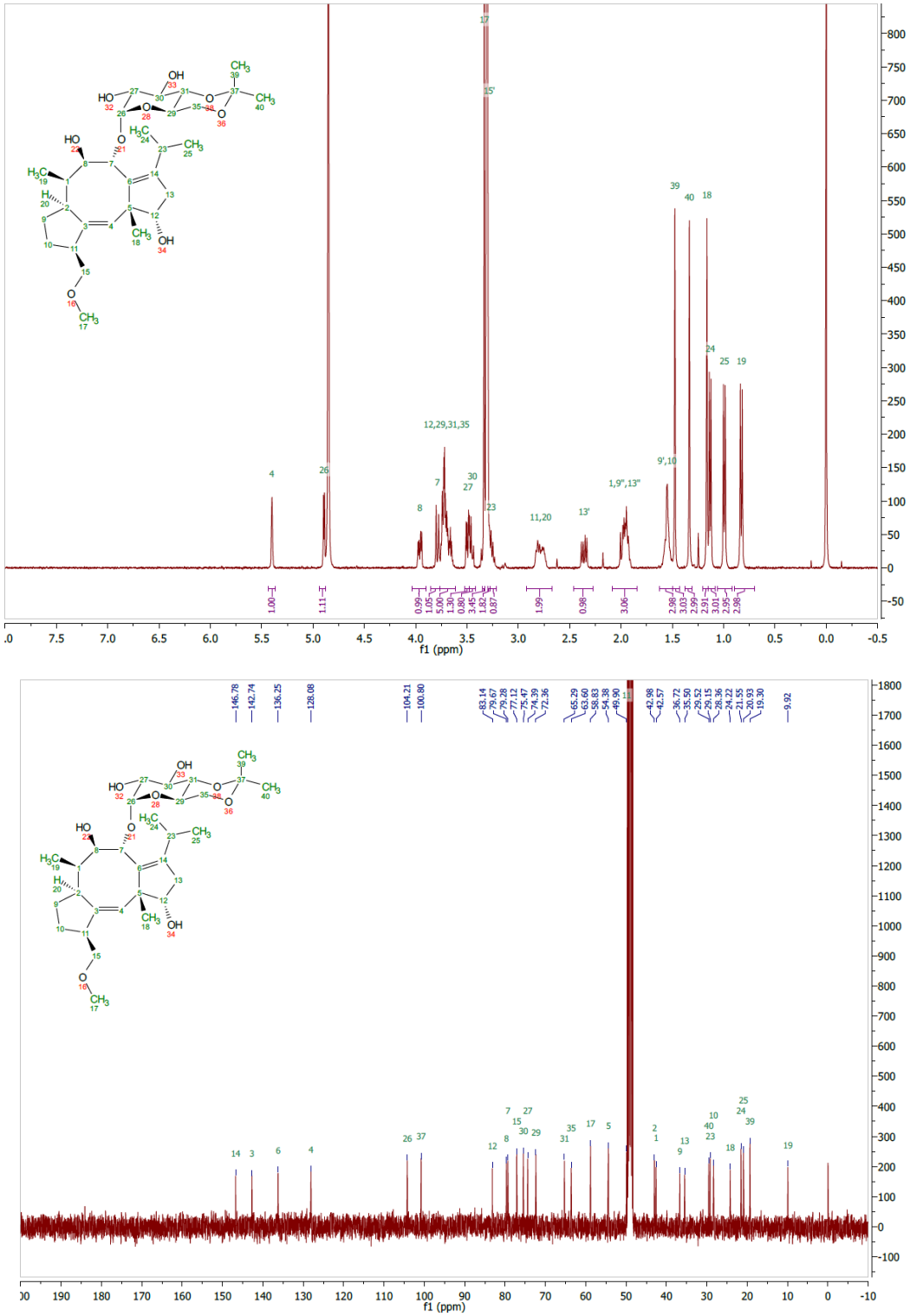

Supporting Figure 18. ^{1}H and ^{13}C NMR spectra of **FC-J Acetonide** in CD_3OD.

References

1. Stevers, L. M. *et al.* Characterization and small-molecule stabilization of the multisite tandem binding between 14-3-3 and the R domain of CFTR. *Proc. Natl. Acad. Sci.* **113**, 1152-1161; (2016).
2. Anders, C. *et al.* A Semisynthetic Fusicoccane Stabilizes a Protein-Protein Interaction and Enhances the Expression of K+ Channels at the Cell Surface. *Chem. Biol.* **20**, 583–593 (2013).
3. Ottmann, C. *et al.* Phosphorylation-independent interaction between 14-3-3 and exoenzyme S: from structure to pathogenesis. *EMBO J.* **26**, 902–913 (2007).
4. Inoue, T. *et al.* Semisynthesis and biological evaluation of a cotylenin A mimic derived from fusicoccin A. *Bioorg. Med. Chem. Lett.* **28**, 646–650 (2018).
5. Andrei, S. A. *et al.* Rationally Designed Semisynthetic Natural Product Analogues for Stabilization of 14-3-3 Protein–Protein Interactions. *Angew. Chem. Int. Ed.* **57**, 13470–13474 (2018).
6. Kim, Y.-W., Grossmann, T. N. & Verdine, G. L. Synthesis of all-hydrocarbon stapled [alpha]-helical peptides by ring-closing olefin metathesis. *Nat Protoc.* **6**, 761–771 (2011).
7. Doveston, R. G. *et al.* Small-molecule stabilization of the p53 – 14-3-3 protein-protein interaction. *FEBS Lett.* **591**, 2449–2457 (2017).
8. Bier, D. *et al.* Molecular tweezers modulate 14-3-3 protein–protein interactions. *Nat Chem* **5**, 234–239 (2013).
9. Milroy, L.-G. *et al.* Stabilizer-Guided Inhibition of Protein–Protein Interactions. *Angew. Chem. Int. Ed.* **54**, 15720–15724 (2015).
10. den Hamer, A. *et al.* Small-Molecule-Induced and Cooperative Enzyme Assembly on a 14-3-3 Scaffold. *ChemBioChem* **18**, 331–335 (2017).
11. Leeuwen, I. J. D. V. *et al.* Interaction of 14-3-3 proteins with the Estrogen Receptor Alpha F domain provides a drug target interface. *Proc. Natl. Acad. Sci.* **110**, 8894–8899 (2013).
12. Ottmann, C. *et al.* Structure of a 14-3-3 Coordinated Hexamer of the Plant Plasma Membrane H+-ATPase by Combining X-Ray Crystallography and Electron Cryomicroscopy. *Mol. Cell* **25**, 427–440 (2007).